Marian Hebenbrock*, Soňa Gurská, Kateřina Bogdanová, Kristýna Rešová, Milan Kolář, Felix Boisten, Marián Hajdúch, Petr Džubák and Jens Müller

Cytotoxicity and antimicrobial activity of platinum(II) complexes based on the ligand precursor 2-phenyl-6-(1,2,3-triazol-4-yl)pyridine – influence of substituent and ancillary ligand on selectivity and activity

https://doi.org/10.1515/znc-2025-0262
Received November 4, 2025; accepted April 15, 2026;
published online June 1, 2026

Abstract: The development of metal-based anticancer agents has been a significant area of research since the discovery of cisplatin's cytostatic effects. In this study, we investigate the cytotoxicity of tridentate ligands derived from 2-phenyl-6-(1,2,3-triazol-4-yl)pyridine and their platinum(II) and palladium(II) complexes against various human cancer cell lines and normal fibroblasts. Several complexes exhibit high cytotoxicity, particularly against acute T-lymphoblastic leukemia cells (CCRF-CEM). Notably, a platinum(II) complex containing an acylpyrrolidine ligand demonstrates remarkable cancer cell selectivity with a submicromolar IC_{50} value of 0.17 μM. Cell cycle analysis revealed that these compounds induce apoptosis and affect DNA/RNA synthesis. Additionally, some complexes show significant antimicrobial activity against Gram-positive bacteria and yeast. Our findings highlight the potential of these metal complexes as selective anticancer agents and underscore the importance of further mechanistic studies.

Keywords: cytotoxicity; platinum(II) complexes; tridentate ligands; metalation

1 Introduction

While the origins of chemotherapy trace back to organic alkylating agents [1, 2], the triumph of modern metal-based drugs began with the serendipitous discovery of the cytostatic effects of cisplatin [3, 4]. Even today, cisplatin represents an important anticancer drug [5]. Despite this success, the emergence of resistance to cisplatin treatment necessitated the development of second-generation platinum-based drugs [6]. In addition, the quest for metal-based drugs with a mode of action different from that of cisplatin led to the development of numerous other biologically active metal complexes [7]. Over the course of several decades, platinum complexes either conceptually similar to cisplatin or structurally entirely different platinum compounds were identified as suitable candidates for chemotherapy [8–11]. These complexes typically exhibit a mode of action distinct from that of cisplatin [12, 13].

Aside from their relevance in the field of medicinal inorganic chemistry, platinum(II) complexes in general are also of enormous interest as luminescent materials [14–16]. As part of the development of luminescent compounds for a potential use in imaging applications, we recently identified compounds with an (undesired) increased cytotoxicity during a screening of their toxicological parameters [17]. In these compounds, the central platinum(II) ion is coordinated by a tridentate CˆNˆN or CˆCˆN donor ligand derived from 2-phenyl-6-(1,2,3-triazol-4-yl)pyridine (Chart 1). The square planar coordination environment is completed by a monodentate ancillary ligand.

***Corresponding author: Marian Hebenbrock**, Institute of Inorganic and Analytical Chemistry, University of Münster, Corrensstr. 28/30, 48149 Münster, Germany, E-mail: hebenbro@uni-muenster.de. https://orcid.org/0000-0002-9339-5165

Soňa Gurská, Marián Hajdúch and Petr Džubák, Faculty of Medicine and Dentistry, Institute of Molecular and Translational Medicine, Palacký University and University Hospital Olomouc, Hněvotínská 1333/5, 779 00, Olomouc, Czech Republic; and Institute of Molecular and Translational Medicine, Czech Advanced Technology and Research Institute (CATRIN), Palacký University Olomouc, Hněvotínská 1333/5, 779 00, Olomouc, Czech Republic

Kateřina Bogdanová, Kristýna Rešová and Milan Kolář, Department of Microbiology, Faculty of Medicine and Dentistry, Palacký University, Hněvotínská 3, 775 15, Olomouc, Czech Republic

Felix Boisten and Jens Müller, Institute of Inorganic and Analytical Chemistry, University of Münster, Corrensstr. 28/30, 48149 Münster, Germany. https://orcid.org/0000-0003-4713-0606 (J. Müller)

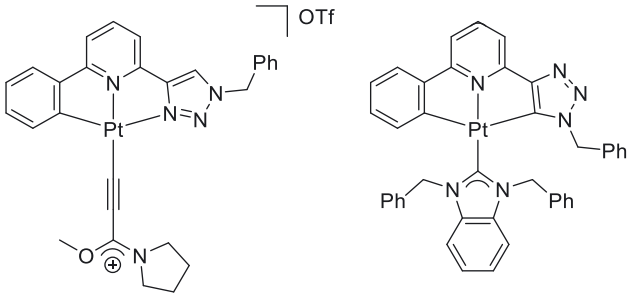

Chart 1: Examples of recently reported cytotoxic, luminescent platinum(II) complexes [17].

These complexes differ from cisplatin in various ways. Most importantly, they bear one tridentate aromatic ligand and one monodentate ligand. This ancillary ligand can either act as a leaving group (e.g., Cl^-, I^-) or engage in a kinetically inert metal–ligand bond (e.g., C, N, or P donor). In contrast, cisplatin contains four monodentate inorganic ligands, two of which function as leaving groups, resulting in its well-established binding to DNA via two coordinate bonds [5]. The general composition of the complexes investigated here indicates that their cytotoxic effect is based on a mode of action different from that of cisplatin and its derivatives. Investigations of the cytotoxicity of other cyclometalated platinum complexes, some of which also demonstrate cytotoxic activity in cisplatin-resistant cells, are supportive of this assumption [18–29].

The presence of an aromatic ligand in the metal complexes offers alternative binding modes, such as intercalation and groove binding [30, 31]. In addition to targeting double-stranded DNA, square-planar metal complexes are known to be able to interact with tetra-stranded guanine quadruplex DNA, either via π stacking or by coordination to a guanine residue [32]. Interestingly, platinum(II) complexes containing the CˆNˆN ligand used here were previously shown to engage in these types of interaction with DNA. Depending on the identity of the substituents on the tridentate ligand and the identity of the ancillary ligand, groove binding to double-stranded DNA and an interaction with quadruplex DNA can be triggered, respectively [33–35]. While complexes with long alkyl tethers favor groove binding, small substituents and essentially planar molecules prefer quadruplex binding [33–35]. Intercalation into duplex DNA appears less likely due to the small size of the CˆNˆN ligand compared to classical metallo-intercalators [36], even though it cannot be ruled out completely [37]. As a result of different possible modes of action, slight variations in the substitution pattern of the tridentate ligand and in the identity of the ancillary ligand are expected to result in different biological properties of the complexes.

Due to their common d^8 electronic configuration, platinum(II) and palladium(II) complexes adopt closely related structures. Nevertheless, the biological properties of these complexes can differ significantly [38–40]. The differences often arise from an increased lability (and hence faster deactivation) of the palladium(II) complex [20]. In this context, the use of a tridentate ligand significantly enhances the palladium(II) complex stability [20].

These considerations served as motivation to delve more deeply into the investigation of platinum(II) complexes based on our tridentate ligands. We therefore set out to evaluate the cytotoxicity against various cancer cell lines and normal fibroblasts. Additionally, we assessed the antimicrobial activity of these compounds and investigated their effects on cell cycle progression and apoptosis. In addition to platinum(II) complexes derived from our previously reported compounds [17], analogous Pd(II) complexes were also generated and evaluated. Moreover, serving as a reference, the ligand precursors of the tridentate ligands were tested for their cytotoxic properties, too.

2 Experimental

2.1 Materials and methods

NMR spectra were recorded on Bruker Avance(III) 400, Avance NEO 400, and Avance NEO 500 instruments. NMR spectra were referenced to residual solvent peaks (CD_3OD, CD_2Cl_2) or to tetramethylsilane ($CDCl_3$). Elemental analyses were performed on a Vario EL III CHNS analyser.

2.2 Synthesis of the *para*-toluoyl-protected deoxyribonucleoside 1b

The β-azido sugar **III** [41] (414 mg, 1.13 mmol) was dissolved together with 2-ethynyl-6-phenylpyridine [42] (150 mg, 1.13 mmol, 1.0 equiv.) in tetrahydrofuran (9 mL) and isopropanol (2.3 mL). Subsequently, copper sulfate pentahydrate (56 mg, 0.23 mmol, 0.2 equiv.) in water (2.3 mL) and sodium ascorbate (112 mg, 0.570 mmol, 0.5 equiv.) were added, and the reaction mixture was stirred at room temperature for 24 h. Ethyl acetate (30 mL) was added, and the organic phase was washed (3 · 20 mL) with an aqueous EDTA solution (0.5 %). The organic phase was dried over magnesium sulfate, and the solvent was removed under vacuum.

The residue was further purified by column chromatography (silica gel, cyclohexane:ethyl acetate, 2:1). The triazole-functionalized 2′-deoxyribose derivative **1b** (364 mg, 0.720 mmol, 64 %) was obtained as a white solid.

^{1}H NMR (400 MHz, $CDCl_3$): δ 8.52 (s, 1 H, $Ar_{Triazole}$-*H*), 8.13 – 8.07 (m, 1 H, $Ar_{Pyridine}$-*H*), 8.04 – 7.98 (m, 2 H, Ar_{Ph}-*H*), 7.98 – 7.93 (m, 2 H, Ar_{Tol}-*H*), 7.89 – 7.80 (m, 3 H, Ar_{Tol}-*H*, $Ar_{Pyridine}$-*H*), 7.71 – 7.64 (m, 1 H, $Ar_{Pyridine}$-*H*), 7.50 – 7.38 (m, 3 H, Ar_{Ph}-*H*), 7.31 – 7.24 (m, 2 H, Ar_{Tol}-*H*), 7.12 – 7.05 (m, 2 H, Ar_{Tol}-*H*), 6.58 (pt, 1 H, H1′), 5.84 – 5.76 (m, 1 H, H3′), 4.75 – 4.57 (m, 3 H, H4′, H5′, H5″), 3.32 – 3.22 (m, 1 H, H2′ or H2″), 2.96 – 2.86 (m, 1 H, H2′ or H2″), 2.44 (s, 3 H, CH_3), 2.28 (s, 3 H, CH_3); **HRMS**: $[C_{34}H_{30}N_4O_5+Na]^+$: calcd. 597.2108, found 597.2123; **EA** ($C_{34}H_{30}N_4O_5$): calcd. C 71.1, H 5.3, N 9.8, found C 71.1, H 5.2, N 9.5.

2.3 Synthesis of complex [2d]

The triazole-based ligand precursor **IV** [42] (100 mg, 0.320 mmol, 1.0 equiv.) was dissolved in acetonitrile (3 mL), and palladium(II) acetate (4 mg, 16 µmol, 5 mol%) along with *N*-iodosuccinimide (100 mg, 0.444 mmol, 1.4 equiv.) were added. The mixture was stirred at 90 °C for 18 h. Water was added, and the reaction mixture was extracted with ethyl acetate. The combined organic phases were dried over magnesium sulfate, and the solvent was removed under reduced pressure. The crude intermediate product was purified by column chromatography on silica gel (cyclohexane:ethyl acetate, 5:1) and isolated as a pale yellow solid (100 mg, 0.228 mmol, 71 %).

^{1}H NMR (400 MHz, $CDCl_3$): δ 8.19 (dd, 1 H, $Ar_{Pyridine}$-*H*, *J* = 7.9, 1.0 Hz), 8.14 (s, 1 H, $Ar_{Triazole}$-*H*), 7.96 (dd, 1 H, Ar_{Ph}-*H*, *J* = 8.0, 1.1 Hz), 7.83 (t, 1 H, $Ar_{Pyridine}$-*H*, *J* = 7.8 Hz), 7.46 (dd, 1 H, Ar_{Ph}-*H*, *J* = 7.6, 1.9 Hz), 7.44 – 7.37 (m, 2 H, Ar_{Ph}-*H*, $Ar_{Pyridine}$-*H*), 7.37 – 7.27 (m, 5 H, Ar_{Benzyl}-*H*), 7.06 (ddd, 1 H, Ar_{Ph}-*H*, *J* = 7.9, 7.2, 1.9 Hz), 5.56 (s, 2 H, CH_2); **{^{1}H}^{13}C NMR** (101 MHz, $CDCl_3$): δ 160.1, 149.6, 148.8, 144.5, 140.0, 136.9, 134.4, 130.2, 129.7, 129.1, 128.7, 128.2, 128.1, 123.2, 122.5, 118.8, 96.7, 54.3; **HRMS**: $[C_{20}H_{15}IN_4+H]^+$: calcd. 439.0414, found 439.0411; **EA** ($C_{20}H_{15}IN_4$): calcd. C 54.8, H 3.5, N 12.8, found C 54.5, H 3.0, N 12.7.

The *o*-iodinated ligand precursor (208 mg, 0.475 mmol, 1.3 equiv.) and bis(dibenzylideneacetone)palladium(0) (210 mg, 0.365 mmol, 1.0 equiv.) were dissolved in dry acetonitrile (5 mL) and stirred at 55 °C for 18 h. Subsequently, the mixture was cooled in an ice bath, and the precipitated solid was filtered off and washed with water, ethanol, and diethyl ether. The product **[2d]** was obtained as a grey-green solid (158 mg, 0.290 mmol, 79 %).

^{1}H NMR (400 MHz, DMF-d_7): δ 9.15 (s, 1 H, $Ar_{Triazole}$-*H*), 8.37 (dd, 1 H, Ar_{Ph}-*H*, *J* = 7.8, 1.2 Hz), 8.13 (t, 1 H, $Ar_{Pyridine}$-*H*, *J* = 7.9 Hz), 7.93 (dd, 1 H, $Ar_{Pyridine}$-*H*, *J* = 8.2, 1.0 Hz), 7.87 (dd, 1 H, $Ar_{Pyridine}$-*H*, *J* = 7.8, 1.0 Hz,), 7.66 (dd, 1 H, Ar_{Ph}-*H*, *J* = 7.7, 1.6 Hz), 7.55 – 7.49 (m, 2 H, Ar_{Benzyl}-*H*), 7.48 – 7.44 (m, 2 H, Ar_{Benzyl}-*H*), 7.44 – 7.40 (m, 1 H, Ar_{Benzyl}-*H*), 7.09 (td, 1 H, Ar_{Ph}-*H*, *J* = 7.4, 1.2 Hz), 6.98 (td, 1 H, Ar_{Ph}-*H*, *J* = 7.5, 1.6 Hz), 5.88 (s, 2 H, CH_2); **{^{1}H}^{13}C NMR** (101 MHz, DMF-d_7): δ 164.3, 153.5, 149.5, 149.1, 147.8, 143.8, 141.4, 135.4, 130.9, 129.7, 129.5, 129.3, 126.0, 125.6, 125.0, 119.0, 119.0, 55.5; **HRMS**: $[C_{20}H_{15}N_4Pd]^+$: calcd. 417.0326, found 417.0334; **EA** ($C_{20}H_{15}IN_4Pd \cdot 1.5\ H_2O$): calcd. C 42.0, H 3.2, N 9.8, found C 42.3, H 2.6, N 9.7.

Single crystals suitable for X-ray structural analysis were obtained by the slow diffusion of benzene into a concentrated solution of the complex in *N*,*N*-dimethylformamide. Those crystals did not contain any co-crystallized solvent.

Crystal Data for **[2d]**: $C_{20}H_{15}IN_4Pd$, M_r = 893.95, yellow needle, 0.31 × 0.14 × 0.12 mm^3, triclinic space group $P\bar{1}$, *a* = 8.8349(3) Å, *b* = 9.1869(3) Å, *c* = 12.5595(4) Å, α = 68.926(2)°, β = 77.548(2)°, γ = 71.039(2)°, V = 893.95(5) Å^3, *Z* = 2, ρ_{calcd} = 2.02 g/cm^3, μ = 2.8 mm^{-1}, F(000) = 524, *T* = 101(2) K, R_1 = 0.0299, wR_2 = 0.0787, 5,281 independent reflections, *S* = 1.075, 235 parameters. CCDC number: 2497809 (Additional information can be found in the SI, Table S2).

2.4 Synthesis of complex [2f]

The hydroxypropyl-functionalized ligand precursor **V** [17] (100 mg, 0.357 mmol, 1.0 equiv.) was dissolved in 2-ethoxyethanol (10 mL) and water (3 mL). The solution was degassed by passing argon through for 30 min. Subsequently, potassium tetrachloridoplatinate (148 mg, 0.357 mmol, 1.0 equiv.) was added, and the mixture was stirred at 90 °C for 18 h. The product was precipitated by adding water, the precipitate was filtered off, and washed with water, ethanol, and diethyl ether. The solid was dried under vacuum, and the product was obtained as a dark green solid (139 mg, 0.273 mmol, 76 %).

^{1}H NMR (400 MHz, DMF-d_7): δ 9.16 (s, 1 H, $Ar_{Triazole}$-*H*), 8.09 (t, 1 H, $Ar_{Pyridine}$-*H*, *J* = 8.0 Hz), 7.86 (dd, 1 H, $Ar_{Pyridine}$-*H*, *J* = 8.2, 1.1 Hz), 7.83 (dd, 1 H, $Ar_{Pyridine}$-*H*, *J* = 7.9, 0.9 Hz), 7.72 (dd, 1 H, Ar_{Ph}-*H*, *J* = 7.6, 1.3 Hz), 7.60 (dd, 1 H, Ar_{Ph}-*H*, *J* = 7.6, 1.5 Hz), 7.17 (td, 1 H, Ar_{Ph}-*H*, *J* = 7.4, 1.5 Hz), 7.09 (td, 1 H, Ar_{Ph}-*H*, *J* = 7.5, 1.4 Hz), 4.82 (t, 1 H, O*H*, *J* = 5.1 Hz), 4.72 (t, 2 H, C–CH_2–N, *J* = 7.1 Hz), 3.64 (q, 2H, O–CH_2–C, *J* = 5.7 Hz), 2.26 – 2.15 (m, 2H, C–CH_2–C); **{^{1}H}^{13}C NMR** (101 MHz, DMF-d_7): δ 166.3, 150.1, 149.0, 147.5, 140.8, 140.7, 134.5, 130.5, 126.9, 125.3, 124.5, 118.3, 118.1, 58.6, 50.1, 33.2; **{^{1}H}^{195}Pt NMR** (86 MHz, DMF-d_7): δ −3,499; **HRMS**: $[C_{16}H_{15}ClN_4OPt + H]^+$: calcd. 510.0655, found 510.0660; **EA** ($C_{16}H_{15}ClN_4OPt$): calcd. C 37.7, H 3.0, N 11.0, found C 37.5, H 2.9, N 10.7.

The hydroxypropyl-functionalized chlorido complex (70 mg, 0.14 mmol, 1.0 equiv.) and tricyclohexylphosphine (59 mg, 0.21 mmol, 1.5 equiv.) were dissolved in acetonitrile (10 mL) and methanol (10 mL) and stirred for 18 h at room temperature. Subsequently, potassium hexafluorophosphate (88 mg, 0.48 mmol, 3.5 equiv.) was added, and the solvent was removed under reduced pressure. The solid was washed with water, extracted with ethanol, and the product was crystallized overnight at −70 °C, washed with a small amount of *n*-pentane, and dried under vacuum. The tricyclohexylphosphine complex was isolated as a yellow solid (115 mg, 0.128 mmol, 91 %).

^{1}H NMR (500 MHz, DMSO-d_6): δ 9.23 (s, 1 H, $Ar_{Triazole}$-*H*), 8.25 (t, 1 H, $Ar_{Pyridine}$-*H*, *J* = 8.0 Hz), 8.10 – 8.04 (m, 1 H, $Ar_{Pyridine}$-*H*), 7.96 (d, 1 H, $Ar_{Pyridine}$-*H*, *J* = 7.7 Hz), 7.75 (dd, 1 H, Ar_{Ph}-*H*, *J* = 7.4, 2.0 Hz), 7.37 (d, 1 H, Ar_{Ph}-*H*, *J* = 7.5 Hz), 7.24 – 7.14 (m, 2 H, Ar_{Ph}-*H*), 4.75 (t, 1 H, O*H*, *J* = 5.0 Hz), 4.65 (t, 2 H, C–CH_2–N, *J* = 7.0 Hz), 3.50 (q, 2 H, O–CH_2–C, *J* = 5.7 Hz), 2.78 (s, 3 H, P–C*H*), 2.11 (p, 2 H, C–CH_2–C, *J* = 6.5 Hz), 2.06 – 1.98 (m, 6 H, CH–CH_2), 1.83 – 1.47 (m, 15 H, CH–CH_2, CH_2–CH_2), 1.39 – 1.13 (m, 9 H, CH_2–CH_2); **{^{1}H}^{13}C NMR** (101 MHz, DMSO-d_6): δ 162.7, 150.9 (d, *J* = 2.9 Hz), 147.9, 146.3, 143.0, 138.3, 133.2 (d, *J* = 6.4 Hz), 131.0, 127.0, 125.8, 125.4, 118.6, 118.1, 57.2, 49.6, 31.9, 31.8, 29.4, 26.8 (d, *J* = 11.4 Hz), 25.8; **{^{1}H}^{195}Pt NMR** (86 MHz, DMSO-d_6): δ −4,080 (d, *J* = 3,727 Hz); **{^{1}H}^{31}P NMR** (202 MHz, DMSO-d_6): δ 23.6, −144.2 (sept, *J* = 711 Hz); **{^{1}H}^{19}F NMR** (471 MHz, DMSO-d_6): δ −70.2 (d, *J* = 711 Hz); **HRMS**: $[C_{34}H_{48}N_4OPPt]^+$: calcd. 754.3208, found 754.3204.

2.5 Synthesis of complex [2h]

The acetonitrile complex **[VI]** [17] (100 mg, 0.151 mmol, 1.0 equiv.) was dissolved in acetonitrile (10 mL), then *tert*-butyl isocyanide (43 µL, 0.38 mmol, 2.5 equiv.) was added, and the reaction mixture was stirred for 1 h at room temperature. Subsequently, potassium hexafluorophosphate (98 mg, 0.53 mmol, 3.5 equiv.) was added. The solvent was removed under vacuum, and the residue was washed with water, ethanol, and diethyl ether. The product was obtained as a red solid (80 mg, 0.11 mmol, 73 %).

^{1}H NMR (400 MHz, DMF-d_7): δ 9.13 (s, 1 H, $Ar_{Triazole}$-*H*), 8.20 (t, 1 H, $Ar_{Pyridine}$-*H*, *J* = 8.0 Hz), 7.94 (d, 1 H, $Ar_{Pyridine}$-*H*, *J* = 8.2 Hz), 7.85 (d, 1 H, $Ar_{Pyridine}$-*H*, *J* = 7.8 Hz), 7.62 (dd, 1 H, Ar_{Ph}-*H*, *J* = 6.3, 2.6 Hz), 7.25 – 7.16 (m, 2 H, Ar_{Ph}-*H*), 7.15 – 7.03 (m, 1 H, Ar_{Ph}-*H*), 4.81 (t, 2 H, C–CH_2–N, *J* = 7.2 Hz), 3.72 (d, 2 H, O–CH_2–C, *J* = 5.9 Hz), 2.28 (p, 2 H, C–CH_2–C, *J* = 6.4 Hz), 1.82 (s, 9 H, CH_3); **{^{1}H}^{13}C NMR** (101 MHz, DMF-d_7): δ 165.4, 151., 149.1, 147.7, 144.8, 137.6, 137.5, 133.1, 128.1, 127.3, 127.1, 120.2, 119.6, 61.1, 58.9, 50.9, 33.4, 30.3; **{^{1}H}^{195}Pt NMR** (86 MHz, DMF-d_7): δ −4,095; **{^{1}H}^{31}P NMR** (202 MHz, DMF-d_7): δ −144.1 (sept, *J* = 710 Hz); **{^{1}H}^{19}F NMR** (471 MHz, DMF-d_7): δ −71.9 (d, *J* = 709 Hz); **HRMS**: $[C_{21}H_{24}N_5OPt]^+$: calcd. 557.1623, found 557.1625.

2.6 Synthesis of complex [2i]

The hydroxypropyl ligand precursor **V** [17] (2.39 g, 8.53 mmol, 1.0 equiv.) was dissolved in *N*,*N*-dimethylformamide. Catalytic amounts of 4-(dimethylamino)pyridine, imidazole (1.45 g, 21.3 mmol, 2.5 equiv.), and triisopropylsilyl chloride (3.1 mL, 15 mmol, 1.7 equiv.) were added, and the mixture was stirred at 50 °C for 18 h. Then, dichloromethane was added, and the mixture was washed three times with water. The solvent was removed under reduced pressure, and the crude product was purified by column chromatography on silica gel (cyclohexane:ethyl acetate + triethylamine, 5:1 + 3 %). The product was obtained as a colorless oil (2.68 g, 6.1 mmol, 72 %).

^{1}H NMR (400 MHz, $CDCl_3$): δ 8.29 (s, 1 H, $Ar_{Triazole}$-*H*), 8.13 (dd, 1 H, $Ar_{Pyridine}$-*H*, *J* = 7.8, 1.0 Hz), 8.07 (d, 2 H, Ar_{Ph}-*H*, *J* = 7.4 Hz), 7.83 (t, 1 H, $Ar_{Pyridine}$-*H*, *J* = 7.8 Hz), 7.67 (dd, 1 H, $Ar_{Pyridine}$-*H*, *J* = 7.9, 1.0 Hz), 7.51 – 7.45 (m, 2 H, Ar_{Ph}-*H*), 7.45 – 7.40 (m, 1 H, Ar_{Ph}-*H*), 4.61 (t, 2 H, C–CH_2–N, *J* = 7.0 Hz), 3.78 (t, 2 H, O–CH_2–C, *J* = 5.7 Hz), 2.19 (ddd, 2 H, C–CH_2–C, *J* = 12.7, 6.9, 5.6 Hz), 1.10 – 1.04 (m, 21 H, C*H*, CH_3); **{^{1}H}^{13}C NMR** (101 MHz, $CDCl_3$): δ 156.8, 150.3, 148.7, 139.2, 137.6, 129.0, 128.7, 126.9, 122.8, 119.3, 118.4, 59.6, 47.2, 33.2, 18.0, 11.9; **{^{1}H}^{29}Si NMR** (79 MHz, $CDCl_3$): δ 13.9; **HRMS**: $[C_{25}H_{36}N_4OSi + H]^+$: calcd. 437.2731, found 437.2720; **EA** ($C_{25}H_{36}N_4OSi$): calcd. C 68.8, H 8.3, N 12.8, found C 68.8, H 8.5, N 12.8.

The TIPS-protected ligand precursor (770 mg, 1.76 mmol, 1.0 equiv.) was dissolved in acetic acid (48 mL). The solution was degassed by passing argon through for 30 min. Subsequently, potassium tetrachloridoplatinate (730 mg, 1.76 mmol, 1.0 equiv.) was added, and the mixture was stirred for 3 d at 120 °C under an argon atmosphere. The precipitated solid was filtered off and washed with water, ethanol, and diethyl ether. The product was obtained as a yellow solid (880 mg, 1.59 mmol, 90 %).

^{1}H NMR (400 MHz, DMF-d_7): δ 9.22 (s, 1 H, $Ar_{Triazole}$-*H*), 8.11 (t, 1 H, $Ar_{Pyridine}$-*H*, *J* = 7.9 Hz), 7.88 (d, 1 H, $Ar_{Pyridine}$-*H*, *J* = 7.9 Hz), 7.85 (d, 1 H, $Ar_{Pyridine}$-*H*, *J* = 7.8 Hz), 7.81 – 7.66 (m, 1 H, Ar_{Ph}-*H*), 7.66 – 7.59 (m, 1 H, Ar_{Ph}-*H*), 7.22 – 7.08 (m, 2 H, Ar_{Ph}-*H*), 4.78 (t, 2 H, C–CH_2–N, *J* = 6.9 Hz), 4.21 (t, 2 H, O–CH_2–C, *J* = 6.1 Hz), 2.46 – 2.35 (m, 2 H, C–CH_2–C), 2.04 (s, 3 H, CH_3); **{^{1}H}^{13}C NMR** (101 MHz, DMF-d_7): δ 171.0, 166.4, 150.2, 149.0, 147.5, 140.7, 140.7, 134.5, 130.6, 126.9, 125.4, 124.6, 118.4, 118.1,

61.8, 50.1, 29.4, 20.7; **{^{1}H}^{195}Pt NMR** (86 MHz, DMF-d_7): δ −3,503; **HRMS**: $[C_{18}H_{17}ClN_4O_2Pt + H]^+$: calcd. 552.0761, found 552.0749; **EA** ($C_{18}H_{17}ClN_4O_2Pt$): calcd. C 39.2, H 3.1, N 10.2, found C 38.8, H 2.9, N 9.9.

2.7 Biology

2.7.1 Cell lines

All cell lines were purchased from the American Tissue Culture Collection (ATCC) except HCT116 and HCT116p53$^{-/-}$ which were obtained from Horizon Discovery. Cells were maintained in TPP 75 cm^2 plastic tissue culture flasks and cultured in media according to ATCC or Horizon recommendations (DMEM/McCoy's 5A modified medium IMDM/EMEM/RPMI 1640 supplemented with 10 % fetal bovine serum and 100 U/ml penicillin-streptomycin). Cells were incubated at 37 °C in a humidified incubator with 5 % CO_2.

2.7.2 Cytotoxicity (MTS assay)

The MTS assay was used to determine the cytotoxic effect of compounds [43–45]. Cell suspensions were prepared and diluted according to the particular cell type to achieve target densities (500 – 4,000 cells/well). Cells (30 µl/well) were seeded into 384-well clear Corning plates using a MultiDrop Combi dispenser (Thermo Fisher Scientific, USA). After 24 h, cells were treated with test compounds, vehicle (DMSO) as a high control, and low/positive controls Actinomycin D (2.67 µM) and Mitomycin C (100 µM) using the ECHO 555 acoustic liquid handler (Labcyte, USA). Compounds were tested at concentrations ranging from 0.012 µM to 50 µM. Treated cells were incubated for 72 h under standard conditions. Following incubation, MTS solution (Promega) was added to cells according to the manufacturer's instructions. After 1 – 4 h, optical density (OD) at 490 nm was measured on a multimode plate reader EnVision (PerkinElmer, USA). Experiments were performed in technical duplicates and at least three biological replicates. The IC_{50} values, the drug concentration lethal to 50 % of the treated cells, were calculated from dose-response curves using the Dotmatics software platform. The assay quality was monitored by determining the Z′-factor for each 384-well plate. The average values of the Z′-factor for individual cell lines were in the range 0.62–0.94.

2.7.3 Cell cycle and apoptosis analysis

Subconfluent CCRF-CEM cells were seeded at a density of $5{\cdot}10^5$ cells·mL^{-1} in 6-well panels and treated with derivatives **1a**, **[2b]**, **[2c]**, **[2e]**, **[2f]**, **[2h]**, and **[3b]**, all of which showed IC_{50} values below 10 µM. Treatments were applied at 1 × or 5 × IC_{50} concentrations for 24 h. Cells were harvested, washed with cold PBS and fixed in 70 % ethanol overnight at −20 °C. The next day, the cells were washed in hypotonic citrate buffer, treated with RNase (50 µg mL^{-1}), stained with propidium iodide, and analyzed by flow cytometry using a 488 nm single beam laser (Becton Dickinson). Cell cycle was analyzed using ModFitLT software (Verity), and apoptosis was measured in a logarithmic model as a percentage of the particles with propidium content lower than cells in G0/G1 phase (<G1) of the cell cycle. Half of the sample was used for $pH3^{Ser10}$ antibody (Sigma) labeling and subsequent flow cytometry analysis of mitotic cells.

2.7.4 BrdU incorporation analysis

Cells were cultured and treated as for cell cycle analysis. Prior to harvesting, cells were pulse-labelled with 10 µM 5-bromo-2′-deoxyuridine (BrdU) for 30 min. Cells were collected by centrifugation (1,500 rpm/5 min/RT), washed with cold 1 × PBS and fixed in ice-cold 70 % ethanol. Following washing with 1 × PBS, cells were incubated in 2M HCl for 30 min at room temperature to denature their DNA. Then, HCl was neutralized with 0.1M $Na_2B_4O_7$ (borax) and cells were washed with 0.5 % Tween-20 and 1 % BSA in 1 × PBS. Further, cell pellets were incubated with a primary anti-BrdU antibody (Exbio) for 30 min at room temperature. Following washing with 1 × PBS, cells were stained with secondary anti-mouse-FITC antibody (Sigma) for 30 min at room temperature in the dark.

The samples were then washed with 1 × PBS and incubated with propidium iodide (0.1 mg/mL) and RNase A (0.5 mg/mL) for 1 h at room temperature in the dark and finally analyzed by flow cytometry (FACSCalibur) using a 488 nm single beam laser.

2.7.5 BrU incorporation analysis

Cells were cultured and treated as for cell cycle analysis. Prior to harvesting, they were pulse-labelled with 1 mM 5-bromouridine (BrU) for 30 min. Then, the cells were fixed in 1 % buffered paraformaldehyde with 0.05 % NP-40 at room temperature for 15 min, followed by incubation at 4 °C overnight. Pelleted cells were washed with 1 % glycine in 1 × PBS followed by washing with 1 × PBS alone. The cells were stained with primary anti-BrdU antibody (Exbio) cross-reacting to BrU for 45 min at room temperature. Following washing with 1 × PBS, the cells were stained with secondary anti-mouse-FITC antibody (Sigma) for 45 min at room temperature in the dark. The cells were washed with 1 × PBS and

fixed with 1 % PBS buffered paraformaldehyde containing 0.05 % NP-40. The samples were then washed with 1 × PBS and incubated with propidium iodide (0.1 mg/mL) and RNase A (0.5 mg/mL) for 1 h at room temperature in the dark. The analysis was performed similarly to the BrdU analysis.

2.7.6 Microbiology

The antimicrobial activity of the tested compounds against aerobic and facultative anaerobic bacteria was assessed using the standard microdilution method determining the minimum inhibitory concentration (MIC) as recommended by EUCAST (European Committee on Antimicrobial Susceptibility Testing). Disposable microtitration plates were used for the tests. The compounds were diluted in an MH II medium (Mueller–Hinton cation adjusted, BioRad, France) and the plates were inoculated with a standard amount of the tested microbe; the inoculum density in each well was equal to 5×10^5 CFU/mL. The plates were incubated for 18 ± 2 h at 35 ± 1 °C, and MICs were determined as the lowest concentration of tested compound that visibly inhibited bacterial growth [46]. The minimum bactericidal concentration (MBC) is characterized as the minimum concentration of the sample required to achieve irreversible inhibition, i.e., killing the bacterium after a defined period of incubation. To determine MBCs, the contents of the wells with visibly inhibited growth were inoculated onto blood agar (Trios, Czech Republic) – 1 µL for each well – and incubated for an additional 18 ± 2 h at 35 ± 1 °C. Negative growth of microbial colonies within the wells with lowest concentration of tested compounds determined the MBCs.

Standard reference bacterial strains (*Enterococcus faecalis* ATCC 29212 = CCM 4224, *Staphylococcus aureus* ATCC 29213 = CCM 4223, *Escherichia coli* ATCC 25922 = CCM 3954, *Pseudomonas aeruginosa* ATCC 27853 = CCM 3955 and *Candida albicans* ATCC 90028 = CCM 8261) from the Czech Collection of Microorganisms (CCM), Faculty of Science, Masaryk University, Brno, were tested with all compounds. Furthermore, in case of antimicrobial activity detection, multi-resistant bacterial strains were also tested, including methicillin-resistant *S. aureus* (MRSA) 4,591/A (PBP2a positive), vancomycin-resistant *Enterococcus faecium* (VRE) VanA phenotype 419/ANA, *Staphylococcus epidermidis* CCM 7221, reference strain for biofilm production (*ica* operon positive), ESBL-positive *E. coli* CE5556 (extended-spectrum beta-lactamase positive strain, CTX-M-15) also resistant to fluoroquinolones (DNA gyrase mutation) and resistant to aminoglycosides, PDC (*Pseudomonas*-derived cephalosporinase)-positive *P. aeruginosa* 21425/C, resistant to beta-lactam antibiotics and fluoroquinolones and *E. coli* 20574, ESBL-positive and resistant to colistin (*mcr* negative).

Strains were obtained from the culture collection of the Department of Microbiology (Faculty of Medicine and Dentistry, Palacký University Olomouc). All tested microorganisms were identified by the MALDI-TOF Biotyper system (Bruker Daltonics, Germany) and stored in cryotubes (ITEST plus, Czech Republic) at −80 °C.

3 Results and discussion

3.1 Syntheses of the complexes

Figure 1 lists the compounds under investigation in this study. Throughout the manuscript, compounds denoted with **1** are non-metalated compounds, compounds marked with **[2]** are metal complexes with a tridentate CˆNˆN ligand, compounds denoted with **[3]** are metal complexes bearing a tridentate CˆNˆC ligand, and compounds denoted with bold Roman numerals are literature-documented precursors. Compounds **1a** [17, 47], **1c** [17], **[2a]** [17, 48], **[2b]** [49], **[2c]** [17], **[2e]** [17], **[2g]** [17], **[2j]** [47], **[2k]** [47], **[3a]** [17], and **[3b]** [17] were synthesized using well-established methods reported in the literature. To broaden the scope of the study, additional platinum(II) complexes of closely related ligands were synthesized. The preparation of the respective ligand precursors was performed as follows.

Ligand precursor **1b** was synthesized analogously to other “click” nucleosides [41, 50–52], starting from 2-deoxy-3,5-di-*O*-(*p*-toluoyl)-β-D-erythro-pentafuranosyl azide **III** [53]. The “click” reaction of the azido sugar was carried out with 2-ethynyl-6-phenylpyridine [42], yielding the *para*-toluoyl-protected deoxyribonucleoside **1b** (Scheme 1).

Complexes **[2d]**, **[2f]**, **[2h]**, and **[2i]** were synthesized from previously reported precursors of the other platinum complexes (Scheme 2): complex **[2d]** was obtained by regioselective palladium(II)-catalyzed iodination of 2-(1-benzyl-1*H*-1,2,3-triazol-4-yl)-6-phenylpyridine **IV** [42] and subsequent oxidative addition of $[Pd(dba)_2]$. Compound **[2f]** was obtained by platination of 3-(4-(6-phenylpyridin-2-yl)-1*H*-1,2,3-triazol-1-yl)propan-1-ol **V** [17] and following substitution of the chlorido ligand by tricyclohexylphosphine. The synthesis of **[2i]** was accomplished by metalating the silyl ether-protected ligand precursor **V** [17]. The introduction of the isocyanido ligand in complex **[2h]** was achieved by replacing the acetonitrile auxiliary ligand in complex **[VI]** [17].

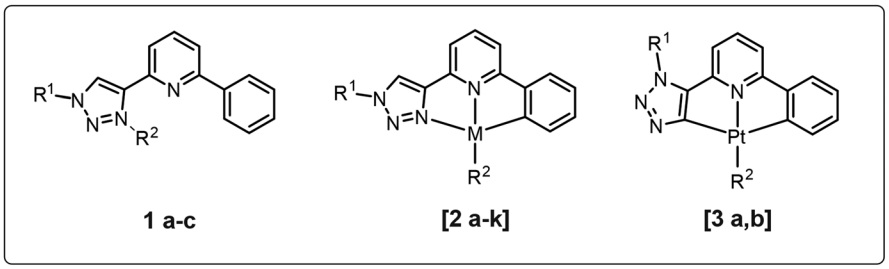

Entry	Cmpd.	R^1	R^2	M	Counterion
1	**1a**	$-(CH_2)_3OH$	–	–	–
2	**1b**	$-^{pTol}$deoxyribose[a]	–	–	–
3	**1c**	$-CH_2Ph$	$-CH_3$	–	BF_4^-
4	**[2a]**	$-CH_2Ph$	–CN	Pt	–
5	**[2b]**	$-CH_2Ph$	$-PPh_3$	Pt	PF_6^-
6	**[2c]**	$-CH_2Ph$	$-CCC(O)N_{pyrrolidin}$	Pt	–
7	**[2d]**	$-CH_2Ph$	–I	Pd	–
8	**[2e]**	$-(CH_2)_3OH$	$-PPh_3$	Pt	PF_6^-
9	**[2f]**	$-(CH_2)_3OH$	$-PCy_3$	Pt	PF_6^-
10	**[2g]**	$-(CH_2)_3OH$	$-NCCH_3$	Pt	PF_6^-
11	**[2h]**	$-(CH_2)_3OH$	$-CNC(CH_3)_3$	Pt	PF_6^-
12	**[2i]**	$-(CH_2)_3OAc$	–Cl	Pt	–
13	**[2j]**	$-(CH_2)_3N_3$	–I	Pt	–
14	**[2k]**	$-(CH_2)_3N_3$	–I	Pd	–
15	**[3a]**	$-CH_2Ph$	–Carbene	Pt	–
16	**[3b]**	$-(CH_2)_3OH$	–Carbene	Pt	–

Figure 1: Compounds under investigation in this study sorted according to their structural backbone. [a] β-D-deoxyribose.

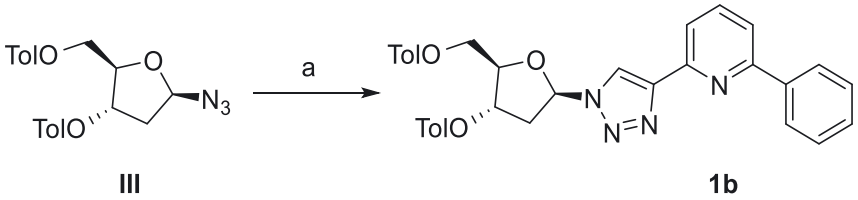

Scheme 1: Synthesis of **1b** starting from the azido sugar **III**. a) 1.0 equiv. 2-ethynyl-6-phenylpyridine, 0.2 equiv. $CuSO_4 \cdot 5\ H_2O$, 0.5 equiv. sodium ascorbate, THF, water, isopropanol, rt, 18 h, 64 %. (Tol- = *para*-toluoyl-).

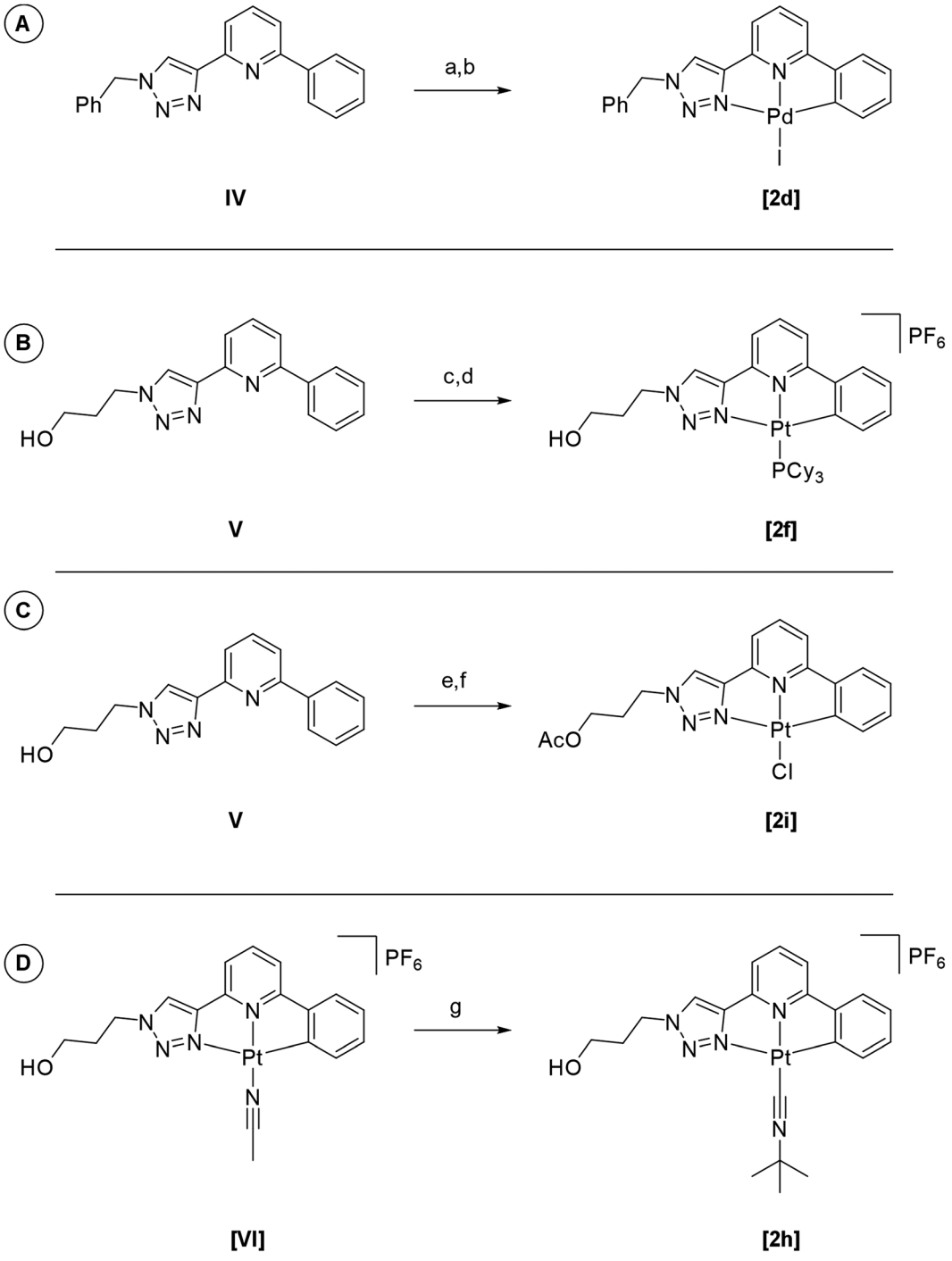

Scheme 2: (A) Synthesis of **[2d]** starting from **IV** [42]: a) 1.4 equiv. NIS, 0.05 equiv. $[Pd(OAc)_2]$, CH_3CN, 90 °C, 18 h, 71 %, b) 0.77 equiv. $Pd(dba)_2$, CH_3CN, 55 °C, 18 h, 78 %; (B) synthesis of **[2f]** starting from ligand precursor **V** [17]: c) 1.0 equiv. K_2PtCl_4, H_2O, DME, 90 °C, 18 h, 76 %, d) 1.5 equiv. PCy_3, CH_3CN, CH_3OH, rt, 18 h, then 3.5 equiv. KPF_6, 91 %; (C) synthesis of **[2i]** starting from compound **V** [17]: e) 1.7 equiv. TIPSCl, 2.5 equiv. imidazole, DMAP, DMF, 50 °C, 18 h, f) 1.0 equiv. K_2PtCl_4, CH_3COOH, 120 °C, 3 d, 90 % over two steps; (D) synthesis of **[2h]** starting from complex **[VI]** [17]: g) 2.5 equiv. $CNC(CH_3)_3$, CH_3CN, rt, 1 h, then 3.5 equiv. KPF_6, 73 %.

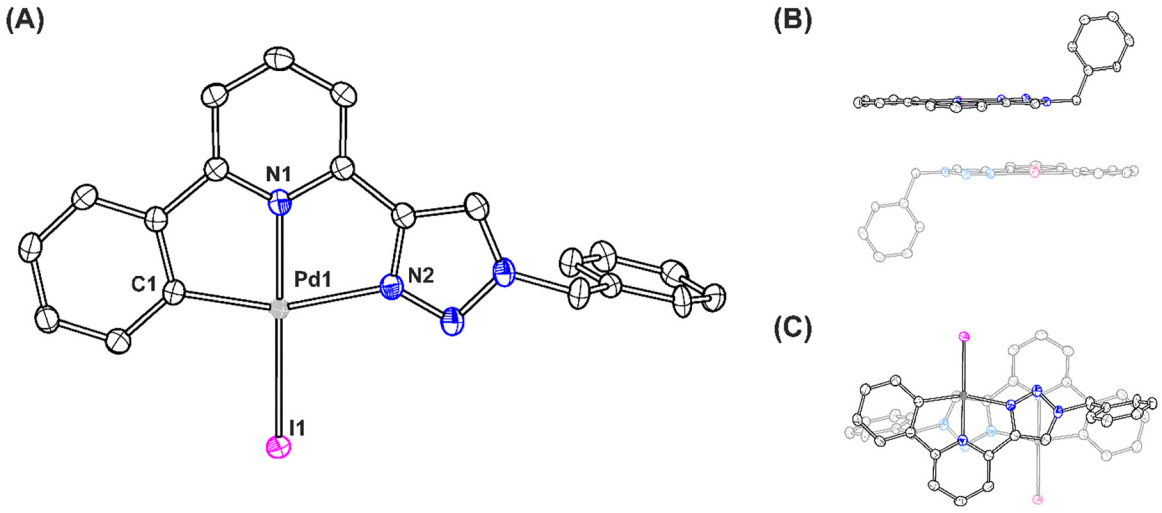

Figure 2: Different views of the molecular structure of **[2d]**. (A) Top view of the (distorted) square-planar coordination environment. (B) Side view of two neighboring complexes, indicating the coplanar stacking. (C) Top view of two neighboring complexes, detailing the coplanar stacking.

3.2 Crystal structure of palladium(II) complex [2d]

By slow diffusion of benzene into a concentrated solution of the palladium(II) complex **[2d]** in *N*,*N*-dimethylformamide, single crystals were obtained, and their molecular structure was elucidated (Figure 2). The compound crystallizes in the triclinic space group $P\,\bar{1}$ with two molecules per unit cell, arranged in a head-to-tail manner. There is no significant interaction between the crystallographically independent molecules apart from coplanar stacking, and the shortest interplanar distance amounts to 3.3 Å.

In the complex, the palladium ion is tetra-coordinated via the tridentate ligand and the iodido ligand resulting in a slightly distorted square-planar coordination geometry. The bond lengths between the coordinating atoms and palladium are as follows: 2.5791(3) Å (Pd1–I1), 2.142(2) Å (Pd1–N2), 1.994(2) Å (Pd1–N1), and 1.986(2) Å (Pd1–C1). They are hence within the normal range [54]. The closest distance between two palladium atoms within the solid-state structure amounts to 5.5159(3) Å, ruling out any metal···metal interaction. The dimeric structure (Figure 2B) formed by π interactions of the ligands resembles that of the closely related platinum(II) complex bearing a monodentate chlorido (rather than iodido) ligand [42]. The striking difference is that in the case of the palladium complex the benzyl substituents point away from each other, whereas in the case of the platinum complex they appear to enclose the dimer structure formed [42].

3.3 Cytotoxicity

All compounds were tested *in vitro* for their cytotoxicity against a panel of six human cancer cell lines (A549: lung adenocarcinoma; CCRF-CEM: acute T-lymphoblastic leukemia; HCT116 and HCT116p53$^{-/-}$: isogenic colon carcinoma lines, p53 wild type and p53 deficient; K562: chronic myelogenous leukemia; U2OS: osteosarcoma), and two noncancerous fibroblast lines (BJ and MRC-5). Of all the compounds tested, only 10 compounds exhibited measurable activity (IC_{50} < 50 µM) in at least one cancer cell line (Table 1). Differences in sensitivity were observed among the individual cell lines, with CCRF-CEM leukemia cells being the most responsive across the compound set. All listed compounds (Figure 3, Table 1) displayed moderate or high cytotoxic effects toward this cell line.

Compounds **1a**, **[2c]**, **[2d]** and **[2k]** showed high selectivity to CCRF-CEM cells. Complex **[2c]** was the most potent, with an IC_{50} of 0.17 µM against CCRF-CEM cells, but no cytotoxicity was detected in other tested cancer cell lines or in normal fibroblasts, indicating a narrow, but highly selective activity profile. The observed cytotoxic activities highlight the different biological response of this leukemia cell line to these compounds and support the hypothesis of cell type-specific mechanism of action. The pronounced sensitivity of CCRF-CEM cells to tested compounds can be attributed to their hematological origin, high proliferative rate, intact apoptotic signaling [55], and limited intrinsic drug-resistance mechanisms [56, 57] compared to solid tumor–derived cell lines.

Table 1: Cytotoxic activity of the most active compounds (IC_{50}, μM) (an overview of the cytotoxicity of all compounds is provided in the SI, Table S1).

Cmpd	CCRF-CEM	K562	A549	U2OS	HCT116	HCT116p53−/−	BJ	MRC-5	TI (all cell lines)	TI (CCRF-CEM)
1a	2.58 ± 0.32	8.89 ± 0.96	10.28 ± 1.83	1.61 ± 0.20	8.31 ± 2.3	6.91 ± 0.76	>50	>50	7.78	19.38
1c	10.51 ± 1.68	>50	>50	>50	>50	>50	>50	>50	1.15	4.76
[2b]	0.30 ± 0.029	1.17 ± 0.06	2.39 ± 0.64	1.24 ± 0.23	3.17 ± 0.52	2.10 ± 0.17	5.76 ± 1.40	6.29 ± 0.93	3.49	20.08
[2c]	0.17 ± 0.32	>50	>50	>50	>50	>50	>50	>50	1.20	294.12
[2d]	26.91 ± 6.24	>50	>50	>50	>50	>50	>50	>50	1.08	1.86
[2e]	0.57 ± 0.047	2.04 ± 0.45	11.49 ± 3.56	3.14 ± 0.45	2.58 ± 0.55	2.24 ± 0.23	6.81 ± 1.17	27.95 ± 5.50	4.73	30.49
[2f]	1.05 ± 0.32	1.29 ± 0.30	4.02 ± 1.00	3.55 ± 0.40	3.20 ± 0.49	3.26 ± 0.48	6.93 ± 0.58	10.72 ± 2.67	3.23	8.40
[2h]	1.97 ± 0.064	>50	15.33 ± 2.46	>50	25.05 ± 4.40	26.54 ± 6.05	>50	>50	1.78	25.38
[2k]	42.43 ± 4.00	>50	>50	>50	>50	>50	>50	>50	1.03	1.18
[3b]	4.94 ± 0.53	9.40 ± 2.20	13.83 ± 2.94	10.19 ± 1.40	10.33 ± 1.51	9.58 ± 1.27	27.06 ± 3.15	36.86 ± 6.61	3.29	6.47

TI (therapeutic index) is calculated as the ratio of mean of IC_{50} values in normal fibroblasts to mean of IC_{50} values in all cancer cell lines or only CCRF-CEM cells.

High cytotoxicity against most cancer cells was observed for compounds **[2b]**, **[2e]**, **[2f]**, and **[3b]**. Again, CCRF-CEM cells showed the lowest IC_{50} values for these compounds. Strong cytotoxic activity of compounds **[2b]**, **[2e]**, and **[2f]** was also observed in another leukemia cell line, K562 (IC_{50} < 10 μM). Solid tumor models were generally less sensitive than leukemia-derived cells, nevertheless, compounds **[2b]**, **[2e]**, and **[2f]** retained significant cytotoxic activity. The cell line HCT116 and its isogenic p53-deficient variant (HCT116 p53−/−) exhibited highly comparable IC_{50} values for most active compounds, suggesting that the cytotoxic effects of these compounds are largely p53-independent in this model. Surprisingly, cytotoxic effects were also observed in the A549 cell line (except for compound **[2e]**), despite the fact that this cell line is characterized by significant resistance to oxidative stress due to constitutive activation of the KEAP1/NRF2 pathway [58]. Importantly, compounds **[2b]**, **[2e]**, and **[2f]** also induced cytotoxic effects in the non-cancer fibroblasts BJ and MRC-5, their IC_{50} values were similar to cancer cells, indicating reduced selectivity toward malignant cells.

In general, the ligand precursor **1a** itself showed high activity against cancer cells (IC_{50} range 1.6–10 μM) without cytotoxicity towards normal cells (therapeutic index – TI 7.78). However, when the ligand precursor **1a** is incorporated into a platinum complex, its specificity in destroying cancer cells is reduced, either the compounds become cytotoxic to non-cancer cells as well (**[2b]**, **[2e]**, and **[2f]**), or the cytotoxicity against all cancer cell lines is reduced (**[2d]** and **[2k]**), with the exception of CCRF-CEM cells (**[2c]** and **[2h]**).

3.4 Cell cycle

The most cytotoxic compounds (IC_{50} < 10 μM for CCRF-CEM cells) were further analyzed for their effects on cell cycle progression and cell death in CCRF-CEM cells after 24 h of treatment at concentrations of 1 × and 5 × IC_{50} (Table 2). All tested compounds induced fragmentation of the nuclei as evidenced by an increased percentage of cells in the sub-G1 phase, particularly at 5 × IC_{50} concentrations. Most compounds caused a slight increase in the G0/G1 phase or S phase cell population. Interestingly, there was a significant decrease in the phosphorylation of histone H3 at serine 10 (marker of mitotic cells), indicating inhibition of mitotic entry. This phenotype is consistent with activation of the G2/M checkpoint, likely a response to DNA damage or replication stress, preventing cells from entering mitosis.

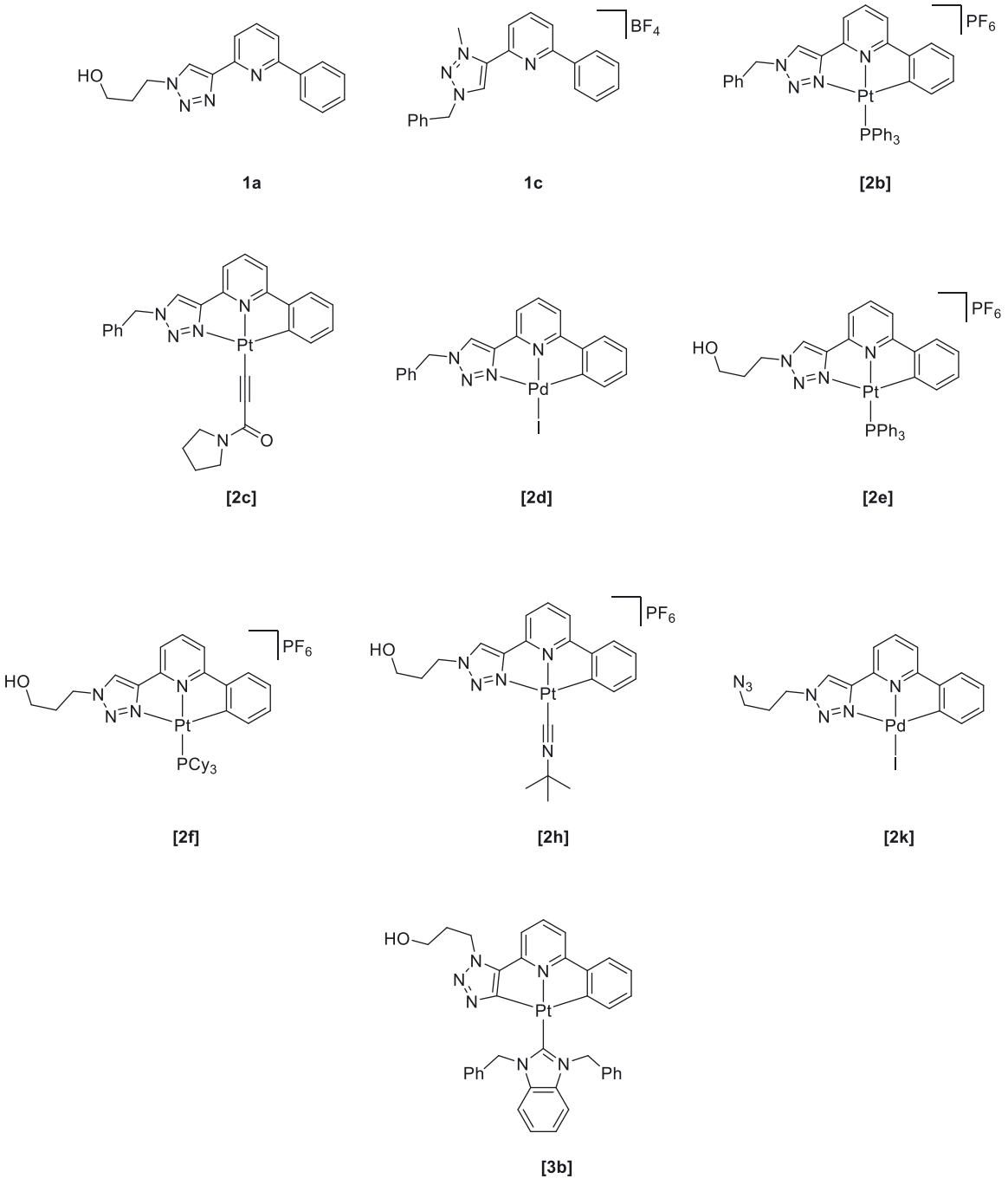

Figure 3: Chemical structures of complexes with noteworthy cytotoxicity (IC_{50} < 50 µM).

Using bromodeoxyuridine (BrdU) and bromouridine (BrU) labeling, we assessed DNA and RNA synthesis activity in drug treated cells. Compounds **[2b]**, **[2e]**, **[2f]** and **[3b]** at $1 \times IC_{50}$ concentrations slightly decreased the intensity of DNA and RNA synthesis, while at $5 \times IC_{50}$, synthesis of both components, DNA and RNA, was nearly stopped. This

Table 2: Effect of active compounds on cell death, cell cycle and DNA/RNA synthesis in CCRF-CEM cell line.

Cmpd	Concentration (µM)		Sub-G1	G0/G1	S	G2/M	>G2/M	M	DNA synthesis	RNA synthesis
Control	–	–	2.92 ± 0.49	41.54 ± 1.91	40.58 ± 0.74	18.10 ± 1.62	11.40 ± 0.34	1.61 ± 0.17	45.25 ± 1.02	40.65 ± 0.85
1a	1 × IC_{50}	2.58	5.00 ± 0.14	33.16 ± 3.95	53.18 ± 4.11	13.66 ± 0.99	14.33 ± 0.99	1.18 ± 0.02	46.33 ± 3.26	43.05 ± 1.95
	5 × IC_{50}	12.90	11.00 ± 0.57	49.84 ± 0.29	40.64 ± 1.22	9.52 ± 1.21	9.92 ± 0.79	0.26 ± 0.04	39.96 ± 2.82	34.78 ± 1.92
[2b]	1 × IC_{50}	0.30	11.40 ± 2.42	46.06 ± 0.49	39.72 ± 2.6	13.89 ± 1.90	13.42 ± 1.24	1.80 ± 0.09	43.91 ± 0.42	46.12 ± 3.63
	5 × IC_{50}	1.50	18.57 ± 1.06	40.10 ± 0.81	46.18 ± 2.85	13.72 ± 2.34	12.72 ± 0.42	1.45 ± 0.09	26.50 ± 2.27	0.33 ± 0.77
[2c]	1 × IC_{50}	0.17	3.81 ± 0.54	36.26 ± 1.62	49.51 ± 2.45	14.23 ± 1.98	14.72 ± 3.77	2.80 ± 0.30	47.62 ± 0.79	47.14 ± 0.10
	5 × IC_{50}	0.85	5.61 ± 0.17	41.21 ± 2.37	43.47 ± 1.99	15.33 ± 0.95	12.76 ± 0.46	3.53 ± 0.23	54.73 ± 1.38	39.21 ± 2.48
[2e]	1 × IC_{50}	0.57	5.48 ± 0.65	43.93 ± 2.19	42.68 ± 2.82	13.39 ± 1.53	11.05 ± 0.32	1.54 ± 0.13	44.03 ± 0.51	29.18 ± 3.25
	5 × IC_{50}	2.85	10.89 ± 0.36	39.06 ± 0.63	42.52 ± 1.12	18.42 ± 0.75	14.16 ± 0.54	0.60 ± 0.10	10.75 ± 2.36	2.06 ± 1.05
[2f]	1 × IC_{50}	1.05	5.48 ± 0.05	54.97 ± 1.25	31.47 ± 0.30	13.56 ± 0.99	10.89 ± 0.40	0.97 ± 0.05	37.25 ± 1.37	41.75 ± 0.58
	5 × IC_{50}	5.25	21.15 ± 1.76	35.77 ± 1.89	48.19 ± 1.33	16.04 ± 2.22	13.55 ± 0.21	0.78 ± 0.15	0.69 ± 0.13	0.70 ± 0.26
[2h]	1 × IC_{50}	1.97	5.95 ± 0.36	44.14 ± 0.50	43.37 ± 0.45	12.49 ± 0.92	14.15 ± 0.30	1.09 ± 0.05	53.02 ± 6.16	36.95 ± 5.71
	5 × IC_{50}	9.85	10.37 ± 1.02	43.15 ± 1.26	42.20 ± 2.34	14.65 ± 1.73	14.40 ± 0.33	1.22 ± 0.10	22.33 ± 1.04	30.66 ± 2.13
[3b]	1 × IC_{50}	4.94	5.56 ± 0.18	43.68 ± 1.37	42.38 ± 0.64	14.03 ± 0.60	15.08 ± 0.59	1.15 ± 0.12	23.89 ± 0.71	39.94 ± 0.10
	5 × IC_{50}	24.70	10.63 ± 0.63	47.92 ± 1.28	38.18 ± 1.35	13.90 ± 1.31	11.85 ± 0.18	0.99 ± 0.12	6.13 ± 0.26	2.19 ± 1.91

complete shutdown of nucleic acid synthesis at high concentration indicates that the complex interferes with fundamental processes like DNA replication or transcription.

3.5 Antimicrobial activity

Antimicrobial activity of the compounds was tested against Gram-positive bacteria (*S. aureus* CCM 4223, methicillin-resistant *S. aureus* (MRSA) 4,591, *S. epidermidis* CCM 7221, *E. faecalis* CCM 4224, and vancomycin-resistant *E. faecium* 419/ANA), Gram-negative bacteria (*E. coli* CCM 3954, ESBL-positive *E. coli* CE 5556, ESBL-positive and resistant to colistin *E. coli* 20574, *P. aeruginosa* CCM 3955, *P. aeruginosa* 21425/C resistant to beta-lactam antibiotics and fluoroquinolones), and yeast (*C. albicans* CCM 8261). Inhibitory activities presented in Table 3 are expressed as minimal bactericidal concentration (MBC) and minimal inhibitory concentration (MIC). Compounds **[2b]**, **[2e]**, **[2f]**, **[2i]**, **[2j]** and **[2k]** exhibited inhibitory activity against all tested Gram-positive bacterial strains, with compounds **[2b]**, **[2e]** and **[2f]** showing MICs below 10 µM. Compound **[2k]** showed strong inhibition of *S. epidermidis* but was less potent against other Gram-positive strains. Compounds **[2i]** and **[2j]** showed weak selective activity against *Staphylococcus* sp. strains. Except for compound **[2e]**, which inhibited Gram-negative bacteria at 50 µM, the compounds were inactive against Gram-negative strains. *C. albicans* was highly sensitive to compounds **[2e]** and **[2f]**.

The data allow some comparisons between structurally related compounds. For example, complexes **[2j]** and **[2k]** only differ by the identity of their central metal ion (Pt vs. Pd), yet the palladium complex is significantly more active against Gram-positive bacteria. This trend in activity correlates with the larger lability of palladium complexes, suggesting that their mode of action involves the dissociation of the iodido ligand. Similarly, a comparison of the activity of the platinum complexes **[2a]**, **[2b]**, and **[2c]**, which contain the same C^N^N ligand but different monodentate ligands, shows activity against Gram-positive bacteria and yeast for **[2b]** only. This complex stands out in that it is the only ionic compound among the three complexes. However, its activity is more likely due to its PPh_3 ligand, as a comparison within the complexes **[2e]**–**[2h]** shows. All of these four complexes are ionic, yet only **[2e]** and **[2f]** bearing phosphine ligands show activity against Gram-positive bacteria. Hence, an involvement of the phosphine in the mechanism of action is likely.

Table 3: Antimicrobial activity of active compounds (MIC and MBC in μM; n/a, not active).

Cmpd.	Gram-positive bacterial strains										Gram-negative bacterial strains										Yeast	
	S. aureus CCM 4223		*S. aureus* MRSA 4591		*Staphylococcus epidermidis* CCM 7221		*E. faecalis* CCM 4224		*Enterococcus faecium* 419/ANA		*Escherichia coli* CCM 3954		*E. coli* CE5556		*E. coli* 20574		*Pseudomonas aeruginosa* CCM 3955		*P. aeruginosa* R		*C. albicans* CCM 8261	
	MIC (μM)	MBC (μM)	MIC (μM)	MBC (μM)	MIC (μM)	MBC (μM)	MIC (μM)	MBC (μM)	MIC (μM)	MBC (μM)	MIC (μM)	MBC (μM)	MIC (μM)	MBC (μM)	MIC (μM)	MBC (μM)	MIC (μM)	MBC (μM)	MIC (μM)	MBC (μM)	MIC (μM)	MBC (μM)
1a	>200	>200	n/a	n/a	n/a	n/a	>200	>200	n/a	n/a	>200	>200	n/a	n/a	n/a	n/a	>200	>200	n/a	n/a	200	>200
1b	>200	>200	n/a	n/a	n/a	n/a	>200	>200	n/a	n/a	>200	>200	n/a	n/a	n/a	n/a	>200	>200	n/a	n/a	>200	>200
1c	200	200	>200	>200	>200	>200	>200	>200	n/a	n/a	>200	>200	n/a	n/a	n/a	n/a	>200	>200	n/a	n/a	>200	>200
[2a]	>200	>200	n/a	n/a	n/a	n/a	>200	>200	n/a	n/a	>200	>200	n/a	n/a	n/a	n/a	>200	>200	n/a	n/a	>200	>200
[2b]	3.13	3.13	3.13	3.13	3.13	3.13	6.25	6.25	6.25	6.25	>200	>200	n/a	n/a	n/a	n/a	>200	>200	n/a	n/a	6.25	6.25
[2c]	>200	>200	n/a	n/a	n/a	n/a	>200	>200	n/a	n/a	>200	>200	n/a	n/a	n/a	n/a	>200	>200	n/a	n/a	>200	>200
[2d]	>200	>200	n/a	n/a	n/a	n/a	>200	>200	n/a	n/a	>200	>200	n/a	n/a	n/a	n/a	>200	>200	n/a	n/a	>200	>200
[2e]	1.56	1.56	3.13	3.13	3.13	3.13	3.13	3.13	3.13	6.25	50	>200	50	>200	50	>200	50	>200	50	>200	3.13	3.13
[2f]	3.13	3.13	3.13	3.13	1.56	1.56	6.25	6.25	6.25	6.25	>200	>200	n/a	n/a	n/a	n/a	>200	>200	n/a	n/a	6.25	6.25
[2g]	>200	>200	n/a	n/a	n/a	n/a	>200	>200	n/a	n/a	>200	>200	n/a	n/a	n/a	n/a	>200	>200	n/a	n/a	>200	>200
[2h]	>200	>200	n/a	n/a	n/a	n/a	>200	>200	n/a	n/a	>200	>200	n/a	n/a	n/a	n/a	>200	>200	n/a	n/a	200	200
[2i]	50	100	200	>200	50	200	>200	>200	n/a	n/a	>200	>200	n/a	n/a	n/a	n/a	>200	>200	n/a	n/a	>200	>200
[2j]	50	100	50	50	25	25	>200	>200	n/a	n/a	>200	>200	n/a	n/a	n/a	n/a	>200	>200	n/a	n/a	>200	>200
[2k]	12.5	12.5	12.5	12.5	3.13	6.25	25	25	25	25	>200	>200	n/a	n/a	n/a	n/a	>200	>200	n/a	n/a	>200	>200
[3a]	>200	>200	n/a	n/a	n/a	n/a	>200	>200	n/a	n/a	>200	>200	n/a	n/a	n/a	n/a	>200	>200	n/a	n/a	>200	>200
[3b]	>200	>200	n/a	n/a	n/a	n/a	>200	>200	n/a	n/a	>200	>200	n/a	n/a	n/a	n/a	>200	>200	n/a	n/a	>200	>200

4 Conclusions

The results presented here underscore the significant potential of tridentate ligands and their metal complexes as cytotoxic agents. Several synthesized compounds exhibit high cytotoxicity against selected cancer cell lines, particularly the platinum(II) complex **[2c]**, bearing a monodentate 1-(pyrrolidin-1-yl)but-2-yn-1-one-4-yl ligand in addition to the common NˆNˆC ligand. This complex demonstrates exceptional selectivity towards CCRF-CEM lymphoblastic leukemia cells with a sub-micromolar IC_{50} value of 0.17 μM and no observed cytotoxicity in normal fibroblasts (therapeutic index 294).

In general, it is observed that while the ligand precursors (e.g., **1a**) of the investigated complexes exhibit cytotoxic properties selectively against cancer cell lines, metalation can enhance cytotoxicity but may reduce selectivity (**[2b]**, **[2e]**, **[2f]**, **[3b]**), resulting in increased effects on normal cells. The observed antimicrobial activity, particularly against Gram-positive bacteria and yeast, broadens the potential therapeutic scope of these complexes.

Further work should focus on elucidating the precise mechanisms of action of the most active metal complexes, to facilitate the rational design of more potent and selective anticancer agents. Investigation into structure-activity relationships and the development of derivatives with improved selectivity is crucial.

Acknowledgments: We acknowledge the contributions from infrastructural projects CZ-OPENSCREEN (LM2023052) and EATRIS-CZ (LM2023053) and from the project National Institute for Cancer Research (Program EXCELES, ID Project No. LX22NPO5102) and IGA_LF_2025_021 and IGA_LF_2025_022. This work was supported by the Technology agency of the Czech Republic project PERMED: T2BA (TN02000109). We thank the German Science Foundation (DFG) for funding (417637295).

Research ethics: Not applicable.

Informed consent: Not applicable.

Author contributions: All authors have accepted responsibility for the entire content of this manuscript and approved its submission.

Use of Large Language Models, AI and Machine Learning Tools: Non declared.

Conflict of interest: The authors declare no conflicts of interest regarding this article.

Research funding: See acknowledgments.

Data availability: Data is available from the corresponding author on well-founded request.

References

1. Wiltshaw E. Cisplatin in the treatment of cancer. Platinum Met Rev 1979;23:90–8.
2. Smith SL. War! what is it good for? Mustard gas medicine. Can Med Assoc J 2017;189:E321–2.
3. Rosenberg B, VanCamp L, Trosko JE, Mansour VH. Platinum compounds: a new class of potent antitumour drugs. Nature 1969;222: 385–6.
4. Rottenberg S, Disler C, Perego P. The rediscovery of platinum-based cancer therapy. Nat Rev Cancer 2021;21:37–50.
5. Lippert B. Cisplatin – chemistry and biochemistry of a leading anticancer drug. Zürich: Verlag Helvetica Chimica Acta 1999.
6. Wang D, Lippard SJ. Cellular processing of platinum anticancer drugs. Nat Rev Drug Discov 2005;4:307–20.
7. Barry NPE, Sadler PJ. Exploration of the medical periodic table: towards new targets. Chem Commun 2013;49:5106–31.
8. Farrer NJ, Woods JA, Salassa L, Zhao Y, Robinson KS, Clarkson G, et al. A potent *trans*-diimine platinum anticancer complex photoactivated by visible light. Angew Chem Int Ed 2010;49:8905–9.
9. Komeda S, Moulaei T, Woods KK, Chikuma M, Farrell NP, Williams LD. A third mode of DNA binding: phosphate clamps by a polynuclear platinum complex. J Am Chem Soc 2006;128:16092–103.
10. Park GY, Wilson JJ, Song Y, Lippard SJ. Phenanthriplatin, a monofunctional DNA-binding platinum anticancer drug candidate with unusual potency and cellular activity profile. Proc Natl Acad Sci USA 2012;109:11987–92.
11. Tsvetkova D, Ivanova S. Application of approved cisplatin derivatives in combination therapy against different cancer diseases. Molecules 2022;27:2466.
12. Ziegler CJ, Silverman AP, Lippard SJ. High-throughput synthesis and screening of platinum drug candidates. J Biol Inorg Chem 2000;5: 774–83.
13. Zhang C, Xu C, Gao X, Yao Q. Platinum-based drugs for cancer therapy and anti-tumor strategies. Theranostics 2022;12:2115–32.
14. Yam VW-W, Law AS-Y. Luminescent d^8 metal complexes of platinum(II) and gold(III): from photophysics to photofunctional materials and probes. Coord Chem Rev 2020;414:213298.
15. Mauro M, Aliprandi A, Septiadi D, Kehr NS, De Cola L. When self-assembly meets biology: luminescent platinum complexes for imaging applications. Chem Soc Rev 2014;43:4144–66.
16. To W-P, Wan Q, Tong GSM, Che C-M. Recent advances in metal triplet emitters with d^6, d^8, and d^{10} electronic configurations. Trends Chem 2020;2:796–812.
17. Maisuls I, Boisten F, Hebenbrock M, Alfke J, Schürmann L, Jasper-Peter B, et al. Monoanionic CˆNˆN luminophores and monodentate C-donor co-ligands for phosphorescent Pt(II) complexes: a case study involving their photophysics and cytotoxicity. Inorg Chem 2022;61:9195–204.
18. Vezzu DA, Lu Q, Chen YH, Huo S. Cytotoxicity of cyclometalated platinum complexes based on tridentate NCN and CNN-coordinating ligands: remarkable coordination dependence. J Inorg Biochem 2014; 134:49–56.
19. Kergreis A, Lord RM, Pike SJ. Influence of ligand and nuclearity on the cytotoxicity of cyclometallated CˆNˆC platinum(II) complexes. Chem Eur J 2020;26:14938–46.
20. Wu S, Wu Z, Ge Q, Zheng X, Yang Z. Antitumor activity of tridentate pincer and related metal complexes. Org Biomol Chem 2021;19:5254–73.

21. Cutillas N, Yellol GS, de Haro C, Vicente C, Rodríguez V, Ruiz J. Anticancer cyclometalated complexes of platinum group metals and gold. Coord Chem Rev 2013;257:2784–97.
22. Quirante J, Ruiz D, Gonzalez A, Lopez C, Cascante M, Cortes R, et al. Platinum(II) and palladium(II) complexes with (N,N') and (C,N,N')-ligands derived from pyrazole as anticancer and antimalarial agents: synthesis, characterization and in vitro activities. J Inorg Biochem 2011; 105:1720–8.
23. Tsai JL, Zou T, Liu J, Chen T, Chan AO, Yang C, et al. Luminescent platinum(ii) complexes with self-assembly and anti-cancer properties: hydrogel, pH dependent emission color and sustained-release properties under physiological conditions. Chem Sci 2015;6:3823–30.
24. Zou T, Liu J, Lum CT, Ma C, Chan RC, Lok CN, et al. Luminescent cyclometalated platinum(II) complex forms emissive intercalating adducts with double-stranded DNA and RNA: differential emissions and anticancer activities. Angew Chem Int Ed 2014;53:10119–23.
25. Cortes R, Crespo M, Davin L, Martin R, Quirante J, Ruiz D, et al. Seven-membered cycloplatinated complexes as a new family of anticancer agents. X-ray characterization and preliminary biological studies. Eur J Med Chem 2012;54:557–66.
26. Garbe S, Krause M, Klimpel A, Neundorf I, Lippmann P, Ott I, et al. Cyclometalated Pt complexes of CNC pincer ligands: luminescence and cytotoxic evaluation. Organometallics 2020;39:746–56.
27. Shi H, Clarkson GJ, Sadler PJ. Dual action photosensitive platinum(II) anticancer prodrugs with photoreleasable azide ligands. Inorg Chim Acta 2019;489:230–5.
28. Dinda J, Adhikary SD, Roymahapatra G, Nakka KK, Santra MK. Synthesis, structure, electrochemistry and cytotoxicity studies of Ru(II) and Pt(II)–N-heterocyclic carbene complexes of CNC-pincer ligand. Inorg Chim Acta 2014;413:23–31.
29. Failes TW, Hall MD, Hambley TW. The first examples of platinum amine hydroxamate complexes: structures and biological activity. Dalton Trans 2003:1596–600. https://doi.org/10.1039/b212553f.
30. Ahmad H, Wragg A, Cullen W, Wombwell C, Meijer AJHM, Thomas JA. From intercalation to groove binding: switching the DNA-binding mode of isostructural transition-metal complexes. Chem Eur J 2014:3089–96. https://doi.org/10.1002/chem.201304053.
31. Lozada IB, Gussakovsky D, Jayawardhana AMDS, McKenna SA, Zheng Y-R, Herbert DE. Photoactive monofunctional platinum(II) anticancer complexes of multidentate phenanthridine-containing ligands: photocytotoxicity and evidence for interaction with DNA. Photochem Photobiol Sci 2023;22:2587–97.
32. Largy E, Hamon F, Rosu F, Gabelica V, De Pauw E, Guédin A, et al. Tridentate N-Donor Palladium(II) complexes as efficient coordinating quadruplex DNA binders. Chem Eur J 2011;17:13274–83.
33. Hebenbrock M, González-Abradelo D, Strassert CA, Müller J. DNA groove-binding ability of luminescent platinum(II) complexes based on a family of tridentate N^N^C ligands bearing differently substituted alkyl tethers. Z Anorg Allg Chem 2018;644:671–82.
34. Guha R, Defayay D, Hepp A, Müller J. Targeting guanine quadruplexes with metal complexes bearing a pendant nucleobase. ChemPlusChem 2021;86:662–73.
35. Kroos S, Hebenbrock M, Hepp A, Layh M, Lüke J, Tonkul AR, et al. Water-soluble luminescent platinum(II) complexes for guanine quadruplex binding. Dalton Trans 2025;54:5367–90.
36. Zeglis BM, Pierre VC, Barton JK. Metallo-intercalators and metallo-insertor. Chem Commun 2007:4565–79. https://doi.org/10.1039/b710949k.
37. Jennette KW, Lippard SJ, Vassiliades GA, Bauer WR. Metallointercalation reagents. 2-Hydroxyethanethiolato(2,2′,2″-terpyridine)-platinum(II) monocation binds srongly to DNA by intercalation. Proc Natl Acad Sci USA 1974;71:3839–43.
38. Akhmetova VR, Bikbulatova EM, Mescheryakova ES, Gil'manova EN, Dzhemileva LU, D'yakonov VA. Synthesis, crystal structure, and in vitro evaluation of the anticancer activity of new Pt (Pd) complexes with 1-[(dimethylamino)methyl]-2-naphthol ligand. Metallomics 2021;13: mfab063.
39. Oliveira LS, Rosa LB, Affonso DD, Santos IA, Da Silva JC, Rodrigues GC, et al. Novel bidentate amine ligand and the interplay between Pd(II) and Pt(II) coordination and biological activity. ChemBioChem 2024;25: e202300696.
40. Romashev NF, Abramov PA, Bakaev IV, Fomenko IS, Samsonenko DG, Novikov AS, et al. Heteroleptic Pd(II) and Pt(II) complexes with redox-active ligands: synthesis, structure, and multimodal anticancer mechanism. Inorg Chem 2022;61:2105–18.
41. Richters T, Krug O, Kösters J, Hepp A, Müller J. A family of "click" nucleosides for metal-mediated base pairing: unravelling the principles of highly stabilising metal-mediated base pairs. Chem Eur J 2014;20:7811–18.
42. Hebenbrock M, Stegemann L, Kösters J, Doltsinis NL, Müller J, Strassert CA. Phosphorescent Pt(II) complexes bearing a monoanionic C^N^N luminophore and tunable ancillary ligands. Dalton Trans 2017; 46:3160–9.
43. Riss TL; Moravec RA; Niles AL; Duellman S; Benink HA; Worzella TJ, et al. Cell viability assays. 2013 May 1 [updated 2016 Jul 1]. In: Sittampalam GS, Coussens NP, Nelson H, et al., editors. Assay Guidance Manual [Online]. Bethesda, MD: Eli Lilly & Company and the National Center for Advancing Translational Sciences, 2004. https://www.ncbi.nlm.nih.gov/books/NBK144065/[Accessed December 10 2016].
44. Borková L, Frydrych I, Jakubcová N, Adámek R, Lišková B, Gurská S, et al. Synthesis and biological evaluation of triterpenoid thiazoles derived from betulonic acid, dihydrobetulonic acid, and ursonic acid. Eur J Med Chem 2020;185:111806.
45. Jurášek M, Řehulka J, Hrubá L, Ivanová A, Gurská S, Mokshyna O, et al. Triazole-based estradiol dimers prepared via CuAAC from 17α-ethinyl estradiol with five-atom linkers causing G2/M arrest and tubulin inhibition. Bioorg Chem 2023;131:106334.
46. The European Committee on Antimicrobial Susceptibility Testing – EUCAST; http://www.eucast.org (Accessed January 1, 2024).
47. Boisten F, Maisuls I, Schäfer T, Strassert CA, Müller J. Site-specific covalent metalation of DNA oligonucleotides with phosphorescent platinum(ii) complexes. Chem Sci 2023;14:2399–404.
48. Sivchik V, Kochetov A, Eskelinen T, Kisel KS, Solomatina AI, Grachova EV, et al. Modulation of metallophilic and pi-pi interactions in platinum cyclometalated luminophores with halogen bonding. Chem Eur J 2021; 27:1787–94.
49. Hebenbrock M, González-Abradelo D, Hepp A, Meadowcroft J, Lefringhausen N, Strassert CA, et al. Influence of the ancillary ligands on the luminescence of platinum(II) complexes with a triazole-based tridentate C^N^N luminophore. Inorg Chim Acta 2021; 516:119988.
50. Litau S, Müller J. A tridentate "click" nucleoside for metal-mediated base pairing. J Inorg Biochem 2015;148:116–20.
51. Richters T, Müller J. A metal-mediated base pair with a [2+1] coordination environment. Eur J Inorg Chem 2014:437–41. https://doi.org/10.1002/ejic.201301491.

52. Hensel S, Eckey K, Scharf P, Megger N, Karst U, Müller J. Excess electron transfer through DNA duplexes comprising a metal-mediated base pair. Chem Eur J 2017;23:10244–8.
53. Štimac A, Kobe J. Stereoselective synthesis of 1,2-*cis*- and 2-deoxyglycofuranosyl azides from glycosyl halides. Carbohydr Res 2000; 329:314–17.
54. Orpen AG, Brammer L, Allen FH, Kennard O, Watson DG, Taylor T. Tables of bond lengths determined by X-Ray and neutron diffraction. Part 2. Organometallic compounds and Co-ordination complexes of the *d*- and *f*-Block metals. J Chem Soc, Dalton Trans 1989:S1–83. https://doi.org/10.1039/dt98900000s1.
55. Geley S, Hartmann BL, Hattmannstorfer R, Löffler M, Ausserlechner MJ, Bernhard D, et al. p53-induced apoptosis in the human T-ALL cell line CCRF-CEM. Oncogene 1997;15:2429–37.
56. Seo SB, Hur JG, Kim MJ, Lee JW, Kim HB, Bae JH, et al. TRAIL sensitize MDR cells to MDR-related drugs by down-regulation of P-glycoprotein through inhibition of DNA-PKcs/Akt/GSK-3β pathway and activation of caspases. Mol Cancer 2010;9:199.
57. Manceau S, Giraud C, Declèves X, Batteux F, Chouzenoux S, Tang R, et al. Lack of P-glycoprotein induction by rifampicin and phenobarbital in human lymphocytes. Int J Pharm 2010;395:98–103.
58. Gong M, Li Y, Ye X, Zhang L, Wang Z, Xu X, et al. Loss-of-function mutations in KEAP1 drive lung cancer progression via KEAP1/NRF2 pathway activation. Cell Commun Signal 2020;18:98.

Supplementary Material: This article contains supplementary material (https://doi.org/10.1515/znc-2025-0262).